



Article

Influence of Ammonia Concentration on Solvay Soda Process Parameters and Associated Environmental and Energetic Effects

Marcin Cichosz ^{1,*}, Urszula Kielkowska ¹, Sławomir Łazarski ^{2,3}, Łukasz Kiedzik ⁴, Marian Szkudlarek ⁴, Kazimierz Skowron ⁴, Beata Kowalska ⁴ and Damian Żurawski ⁴

¹ Department of Chemical Technology, Faculty of Chemistry, Nicolaus Copernicus University in Toruń, 7 Gagarin Street, 87-100 Toruń, Poland

² MCMP Sp. z o.o., 5 Świerkowa Street, 86-300 Grudziądz, Poland

³ Faculty of Civil Engineering and Environmental Sciences, Białystok University of Technology, 45A Wiejska Street, 15-351 Białystok, Poland

⁴ CIECH R&D Sp. z o.o., 62 Wspólna Street, 00-684 Warszawa, Poland

* Correspondence: chemik@umk.pl; Tel.: +48-566-114-787; Fax: +48-566-542-477

Abstract: Modifying the absorption process in soda production by the Solvay method requires performing many calculations and determining a new equilibrium process. An increase in ammonia concentration in the reaction solution causes kinetic changes in equilibrium. Changes to the Solvay soda production technology were determined using chemical and instrumental analysis methods. A modification of the process in the form of SAB was introduced. Information allowing the design of an additional absorber and its location in the network of technological devices was presented in the form of parameters using typical chemical engineering assumptions. Spectroscopic and electrochemical techniques were used for this purpose. The increase in total alkalinity due to the addition of ammonia to 135 mmol·20 cm⁻³ resulted in cooling savings of about 152.4 MJ·Mg⁻¹ of soda. The ammonia desorption rate and process energy parameters were determined for the new system. The temperature requirements for the carbonation column were defined, and in particular, a technique was developed to minimize the cooling of the lower part of the reactor, which reduces the consumption of process energy. Emissions of CO₂ were reduced from 11.70 to 7.85% and NH₃ from 5.52 to 4.89% in exhaust gases from the carbonation column.

Keywords: absorption; ammoniated brine; ammonia-soda industry



Citation: Cichosz, M.; Kielkowska, U.; Łazarski, S.; Kiedzik, Ł.; Szkudlarek, M.; Skowron, K.; Kowalska, B.; Żurawski, D. Influence of Ammonia Concentration on Solvay Soda Process Parameters and Associated Environmental and Energetic Effects. *Energies* **2022**, *15*, 8370. <https://doi.org/10.3390/en15228370>

Received: 3 October 2022

Accepted: 6 November 2022

Published: 9 November 2022

Publisher's Note: MDPI stays neutral with regard to jurisdictional claims in published maps and institutional affiliations.



Copyright: © 2022 by the authors. Licensee MDPI, Basel, Switzerland. This article is an open access article distributed under the terms and conditions of the Creative Commons Attribution (CC BY) license (<https://creativecommons.org/licenses/by/4.0/>).

1. Introduction

The long-term development of the soda industry worldwide has led to a number of modifications to the Solvay process. The main one is the dual process, which allows manufacturing units to produce ammonium chloride (which can be used as a fertilizer) in almost equal amounts as the product. Several plants in the world operate in this mode; most of them are located in China. The Akzo dry lime process, which uses lime instead of lime milk to recover ammonia, is currently considered the most advanced technology. There are technologies in which soda is produced as a by-product [1]. Energy, water consumption, and environmental pollution are a difficult problem in the world. Due to the rapid expansion of technology, the demand for water and energy is increasing, which also enhances the dependence on the availability of these sources [2,3]. The Solvay soda production process is very energy-intensive [4] and is characterized by the large production of solid, liquid, and gaseous waste [5–7]. In many countries worldwide, especially in developing countries, severe water shortages have been caused by population growth, industrialization, global warming, and climate change. Water is the most important resource on Earth, and is essential to human life. It is estimated that approximately 1.8 billion people will be without access to clean drinking water by 2025. The proposed solution in the Solvay soda industry allows for large savings in the consumption of cooling water and energy [8].

There are several energy-consuming processes in the Solvay soda technology: distillation, carbonation (cooling), calcination, and calcination of limestone.

The main issue is the efficiency and energy of the carbonation process of ammoniated brine, especially based on seasonality. In summer, cooling the column is a big challenge. Considering the increasingly higher temperatures and availability of cooling water, this is one of the main economic factors in the operation of a carbonation column. To increase the efficiency of the process when there is less cooling of the column, studies on increasing the concentration of ammonia in the carbonation process were carried out [9].

One of the diffusion operations in the soda production process using the Solvay technique is the absorption of ammonia. Permeation, or mass exchange, is the basis of many unit operations, including distillation, rectification, drying, hydration, absorption, adsorption, crystallization, dissolution, etc. [10]. There is a gap in the research in terms of determining the influence of the ammonia concentration on the efficiency of the soda process under the real conditions of the Solvay process.

Absorption is the uptake of a component or components of a gaseous mixture by a liquid, which is the absorbent. The gas, due to diffusion, penetrates into the liquid through the interfacial surface to form a solution. A gaseous mixture can contain components that are soluble and components that are practically insoluble in the liquid. The former are called active components, the latter neutral or inert [11,12]. This is one of the main processes of Solvay soda technology.

The statics of the absorption process, i.e., the equilibrium between the liquid and the gas phase, depend on the composition of the phases, temperature and pressure, since the two-phase system under consideration has three degrees of freedom according to Gibbs's phase rule [10]. Therefore, at a given temperature and pressure, a fixed composition of one phase corresponds to a well-defined composition of the other phase. Absorption will occur when the content of the component in the gas phase is greater than the corresponding equilibrium state.

Empirical formulas are known in the literature that allow for the approximate determination of the selected parameters of the Solvay process, but their technological usefulness has not been confirmed. Previous research has shown that ensuring the maximum value of the degree of transformation of the sodium ion W_{Na} requires the particularly careful operation of crude brine purification, ammonization, and carbonation.

From the analysis of dependencies, we can formulate:

$$[NH_3, bound] = 68.0 + (c - 95.0) + 0.56((o + e + a + m) - 92.0) + 0.57(R - 190.0) - 0.14(T - 25.0)$$

and

$$W_{Na} = a_1 \cdot R + a_2 \cdot [NH_3, total] + a_3 \cdot [Cl^-]_{total} - a_4 \cdot T$$

It is apparent from the analysis that the figure in question is directly proportional to the value of the degree of carbonation (R) and the concentration of ammonia ($o + e + a + m$) and total sodium chloride (c) in solution (a_1 – a_4 , numerical coeff.). An increase in the temperature of ammoniated brine at the exit from the carbonation column reduces the efficiency of the carbonation process [9].

Previous industrial experience indicates that maintaining the optimal level of process efficiency primarily depends on the magnitude of ammonia desorption in the carbonation apparatus, which is associated with temperature–hydrodynamic conditions and the distribution of the partial pressure of NH_3 over the carbonated ammonia brine solution.

When considering the equation determining the efficiency of the soda process, it should be noted that only one quantity can be changed, taking into account the other parameters. The concentration of chloride ions is the maximum concentration that occurs in saturated brine. The degree of carbonation depends on the amount of CO_2 introduced into the solution and is limited by the amount of $CaCO_3$ decomposition. A change in the concentration of total ammonia remains [13].

The kinetics of absorption, that is, the rate of mass exchange, are determined by how far the system is from equilibrium. Of course, the statics, as well as the kinetics, further depend on the properties of the absorbing liquid, the absorbed component, and the inert gas. The kinetics of the absorption process are also affected by the phase contact conditions, which are related to the design of the absorption device [14].

Absorption is accompanied by a thermal effect caused by a change in state of aggregation [15]. Isothermal absorption is possible when the amount of liquid supplied is large compared to the amount of gas (low solubility of the gas) or when the heat of absorption is properly dissipated from the absorption apparatus; otherwise, the absorption will proceed with a change in the temperature of the system. In many cases, it is difficult to delineate a strict boundary between physical absorption and absorption associated with a chemical reaction [16]. As part of ongoing research at the Inowrocław production plant, it was decided to introduce a new “small” absorber (SAB) to increase the concentration of ammonia in the ammonia brine, pre-carbonated. The optimal operation of the additional absorption process translates into higher utilization of CO₂ and the increased efficiency of the soda process.

First, the input and output parameters of the media for SAB were determined. Second, the number of mass transfer units was calculated, with one mass transfer unit corresponding to a section of the apparatus length over which the change in working concentrations of absorbate equals the average driving force over that section. The absorption process is an exothermic process [14,15].

The height of the mass transfer unit is calculated by the following formula, based on [10]:

$$h_y = \frac{V}{K_v \cdot F_0} \quad (1)$$

The goal of the work carried out was to obtain a stable flux of ammoniated brine, characterized by a direct titer of about 130 mmol·20 cm⁻³ and determine the chloride ion concentration and CO₂ before and after the absorption process.

2. SAB Calculation and Parameters in Modified Process

The main change in the process is the addition of ammonia absorber. This is an essential part of the modification to achieve the stated objectives of this paper. The input parameters of the ammonia brine were as follows: the absorber load was assumed at a level corresponding to 20–30% of the current load of the carbonation column, $V_{\max} = 15\text{--}20 \text{ m}^3 \cdot \text{h}^{-1}$, $C_{\text{NH}_3} \approx 100 \text{ mmol} \cdot 20 \text{ cm}^{-3} \approx 5.00 \text{ mol} \cdot \text{dm}^{-3}$, $C_{\text{NaCl}} \approx 88 \text{ mmol} \cdot 20 \text{ cm}^{-3} \approx 4.40 \text{ mol} \cdot \text{dm}^{-3}$, $T \approx 313 \text{ K}$. The output parameters of ammonia brine with higher ammonia concentration were as follows: $V_{\max} = 15\text{--}20 \text{ m}^3 \cdot \text{h}^{-1}$, $C_{\text{NH}_3} \geq 130 \text{ mmol} \cdot 20 \text{ cm}^{-3} \approx 6.50 \text{ mol} \cdot \text{dm}^{-3}$, $C_{\text{NaCl}} \approx 83 \text{ mmol} \cdot 20 \text{ cm}^{-3} \approx 4.15 \text{ mol} \cdot \text{dm}^{-3}$, $T \approx 333 \text{ K}$.

A general diagram of the proposed absorber to increase the concentration of ammonia in ammonia brine, pre-carbonated, is shown in Figure 1.

An analysis of the adsorbed gas was performed using FT-IR spectroscopy (Vertex 70V FT-IR spectrometer, Bruker Optics, Ettlingen, Germany). The content of 1 Nm³ of the analyzed gas was 0.6482 Nm³ NH₃, 0.1804 Nm³ CO₂, and 0.1714 Nm³ H₂O. The ammonia content of the input gas (bottom of the absorber) was $Y_{\text{down}} = 1.8425 \frac{\text{mol NH}_3}{\text{inerts mol}}$. It was assumed that 90% of ammonia would be absorbed; therefore, $Y_{\text{up } 90} = 0.18425 \frac{\text{mol NH}_3}{\text{inerts mol}}$. The flow rate of the carbonated brine was set at 15–20 m³·h⁻¹, that is, 16,935.0–22,580.0 kg·h⁻¹. The density of the ammonia brine (with values of 100.76 mmol·20 cm⁻³ NH₃ and 89.93 mmol·20 cm⁻³ Cl⁻) was 1.1290 kg·dm⁻³.

Identifying the solution included determining direct alkalinity, total alkalinity (n), the amount of CO₂ (d), and the content of chloride ions (Cl⁻) (c) and ammonium chloride (NH₄Cl) (b).

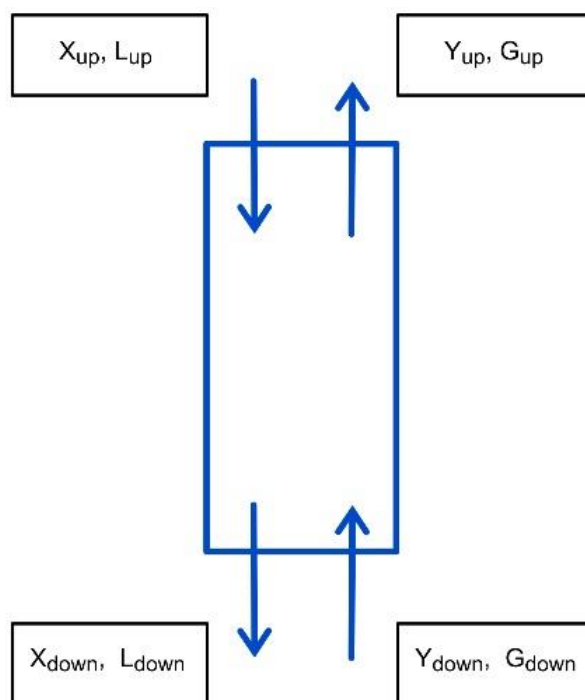


Figure 1. Diagram of absorber and process flux.

The method involves distilling off the ammonia and absorbing it in a standard solution of sulfuric(VI) acid. Excess sulfuric(VI) acid is titrated with a standard solution of sodium hydroxide in the presence of methyl orange. Ammonia contained in liquids in the form of carbonate and bicarbonate salts passes into the gas phase as a result of thermal decomposition of these compounds; this is called free ammonia.

Bound ammonia in the form of NH_4Cl decomposes with a strong alkali such as sodium hydroxide.

2.1. Direct Alkalinity (*n*)

To determine alkalinity, the sample was titrated with 0.5 M sulfuric(VI) acid in the presence of methyl orange. The titration was carried out until the color of the solution changed from yellow to orange-yellow.

2.2. Amount of CO_2 (*d*)

The determination was performed on a Scheibler apparatus. The carbonate and bicarbonate ions contained in the sample were decomposed using hydrochloric acid, with the release of free CO_2 , which displaces the liquid from the gas burette tube so that the amount of gas released can be determined.

2.3. Content of Cl^- (*c*)

The determination of chloride ions was performed using a Metrohm Ti-Touch 916 compact potentiometric titrator. To perform the measurement, the sample was neutralized, then diluted and acidified with sulfuric(VI) acid. The sample was then titrated with 0.03333 M silver nitrate solution in the presence of a silver electrode, using the appropriate instrument software.

2.4. Content of NH_4Cl (*b*)

The potentiometric titrator was used to determine the amount of ammonium chloride in the sample. To carry out the measurement, the sample was boiled in lye; this process involved adding the sample to a specific amount of sodium hydroxide and then leaving it to stand on a hot plate to boil off the ammonia. The remaining excess alkali was titrated with

1 M sulfuric(VI) acid in the presence of a glass electrode, using the appropriate program of the instrument.

2.5. Content of $\text{NH}_2\text{COONH}_4$ (e)

The presence of carbamate ions was confirmed by ^{13}C NMR (Avance 300NMR spectrometer, Bruker, Germany), and the ion content was analyzed using IR spectrometry at a wavelength of 687 cm^{-1} .

All analyses were performed using the standards and methodologies presented in [17].

For the absorption process, based on Whitman–Lewis boundary layer theory and Fick's first law [18], the mass exchange equation can be formulated as:

$$G = K \cdot F \cdot \Delta y \quad (2)$$

The driving force of the mass exchange process can be expressed in terms of difference:

$$\Delta y = (y - y^*) \quad (3)$$

As the absorption process proceeds, the driving force of the mass exchange process changes along the absorption apparatus (i.e., the distance of the system from equilibrium changes). For a sufficiently small mass exchange area dF , the mass exchange equation can be written as:

$$dG = K \cdot dF \cdot (y - y^*) \quad (4)$$

From the material balance, it is known that:

$$G = V \cdot (y_1 - y_2) \text{ or } dG = V dy \quad (5)$$

From the comparison of the above quantities we obtain:

$$dG = K \cdot dF \cdot (y - y^*) = V dy \quad (6)$$

Considering V from the material balance equation, we obtain:

$$K \cdot dF \cdot (y - y^*) = \frac{G}{y_1 - y_2} dy \quad (7)$$

Transforming the equation and integrating the limits from 0 to F and from y_2 to y_1 , we obtain:

$$\int_0^F dF = \frac{G}{y_1 - y_2} \int_{y_2}^{y_1} \frac{dy}{K(y - y^*)} \quad (8)$$

Therefore, we can obtain:

$$G = F \cdot \frac{y_1 - y_2}{\int_{y_2}^{y_1} \frac{dy}{K \cdot (y - y^*)}} = K \cdot F \cdot \Delta y_{sr} \quad (9)$$

where:

$$\Delta y_{sr} = \frac{y_1 - y_2}{\int_{y_2}^{y_1} \frac{dy}{y - y^*}} \quad (10)$$

Most often, however, strict determination of the size of the surface area of the separation of phases is not possible; therefore, in the formulas used for practical calculations, this size is replaced with a readily available volume size. Assuming that the magnitude of the phase separation area is proportional to the volume, we can calculate:

$$F = \alpha \cdot F_0 \cdot H_w \text{ or } dF = \alpha \cdot F_0 \cdot dH_w \quad (11)$$

Eventually, combining the above equations with the basic differential equation, we obtain:

$$dH_w = \frac{V dy}{K_v \cdot F_0 \cdot (y - y^*)} \quad (12)$$

Integrating the above relationship from 0 to H_w and from y_2 to y_1 , we obtain:

$$H_w = \frac{V}{K_v \cdot F_0} \int_{y_2}^{y_1} \frac{dy}{y - y^*} \text{ or, in short, } H_w = h_y m_y \quad (13)$$

As an example, it is useful to present the process of calculating the absorber for water. The solubility of ammonia in water at 313 K at a pressure of 1 atm assuming an isothermal process is shown in Table 1.

Table 1. Solubility of ammonia in water at 313 K at pressure of 1 atm.

$X = \frac{\text{mol NH}_3}{\text{mol H}_2\text{O}}$	$Y = \frac{\text{mol NH}_3}{\text{mol of inert}}$
0.2647	2.3628
0.2117	1.0822
0.1588	0.5605
0.1058	0.2816
0.0794	0.1865
0.0530	0.1112
0.0423	0.0869
0.0318	0.0629
0.0264	0.0520
0.0211	0.0410
0.0169	0.0327
0.0127	0.0246
0.0105	0.0207

We can graph $\frac{(Y_{\text{down}} - Y_{\text{up}})}{(X_{\text{down}}^* - X_{\text{up}})}$, where $X_{\text{up}} = \frac{1.8425 - 0.18425}{(6.5 - 5.0)} = \frac{1.65825}{1.5} = 1.1055 \times 1.2 = 1.3266$; hence, $X_{\text{down}} = 0.2217$. By drawing a graph of $\frac{\text{mol NH}_3}{\text{mol of inert}} = f\left(\frac{\text{mol NH}_3}{\text{mol H}_2\text{O}}\right)$, the number of mass transfer units can be determined graphically, as shown in Figure 2.

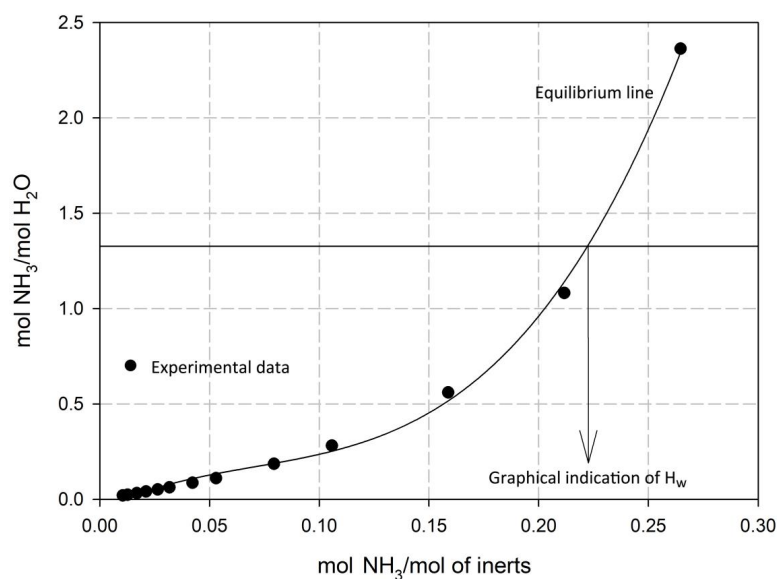


Figure 2. Amount of mass transfer for research absorption system.

The column fill height is the product of the number and height of mass transfer units:

$$H_w = h_y m_y \quad (14)$$

The number of mass transfer units is 0.2217.

We assume that the height of mass penetration for the liquid phase is:

$$h_y = \frac{L}{k_x a S} \quad (15)$$

From here, the parameters of the absorber can be easily calculated.

3. Experimental Results

In order to effectively increase the concentration of ammonia in the pre-carbonated brine, it is necessary to determine the effect of the changes on the solubility of NaCl in the pre-carbonated brine so as not to cause NaCl precipitation.

In order to obtain information on the solubility of NaCl, equilibrium solubility tests were conducted on sodium chloride at 303 K in ammonia solution with equilibrium concentrations of 118 and 106.5 mmol·20 cm⁻³ (initial concentrations 136.5 and 121.6 mmol·20 cm⁻³, respectively), depending on the degree of carbonation of the solution (R). The results of the experiments are shown in Figures 3 and 4.

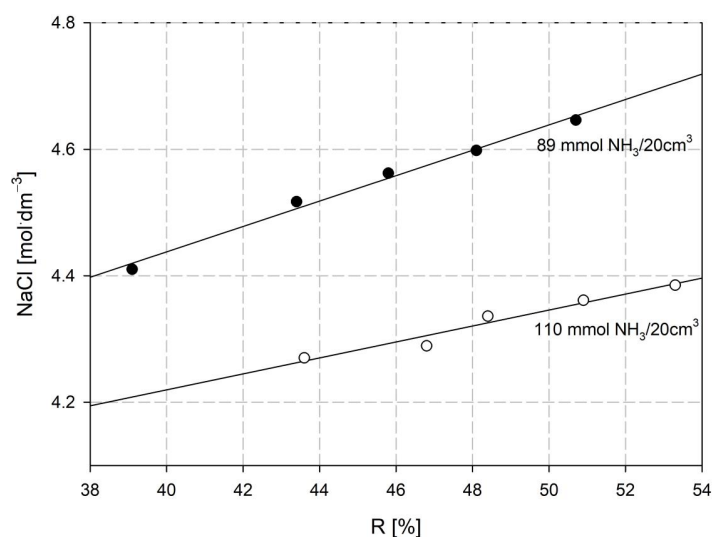


Figure 3. Solubility of NaCl in ammonia solution depending on degree of carbonation.

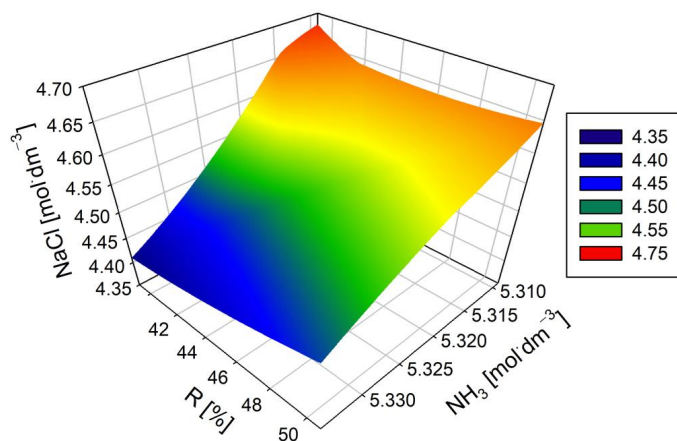


Figure 4. Solubility of NaCl decreases with increasing NH₃ in solution, and simultaneously increases as degree of carbonation of solution rises.

The graphs in Figures 3 and 4 show that the solubility of NaCl decreases with increasing NH_3 in solution, and simultaneously increases as the degree of carbonation of the solution rises. At the same time, the trend of increasing solubility with increasing R is more noticeable. That is, considering the analyzed system, with an increase in the degree of carbonation, the solubility of NaCl increases, and this increase is more characteristic when R is in the range of 42–46%.

The traditional Solvay process absorption system implemented at CIECH Soda Polska S.A.'s Inowroclaw soda plants is shown in Figure 5.

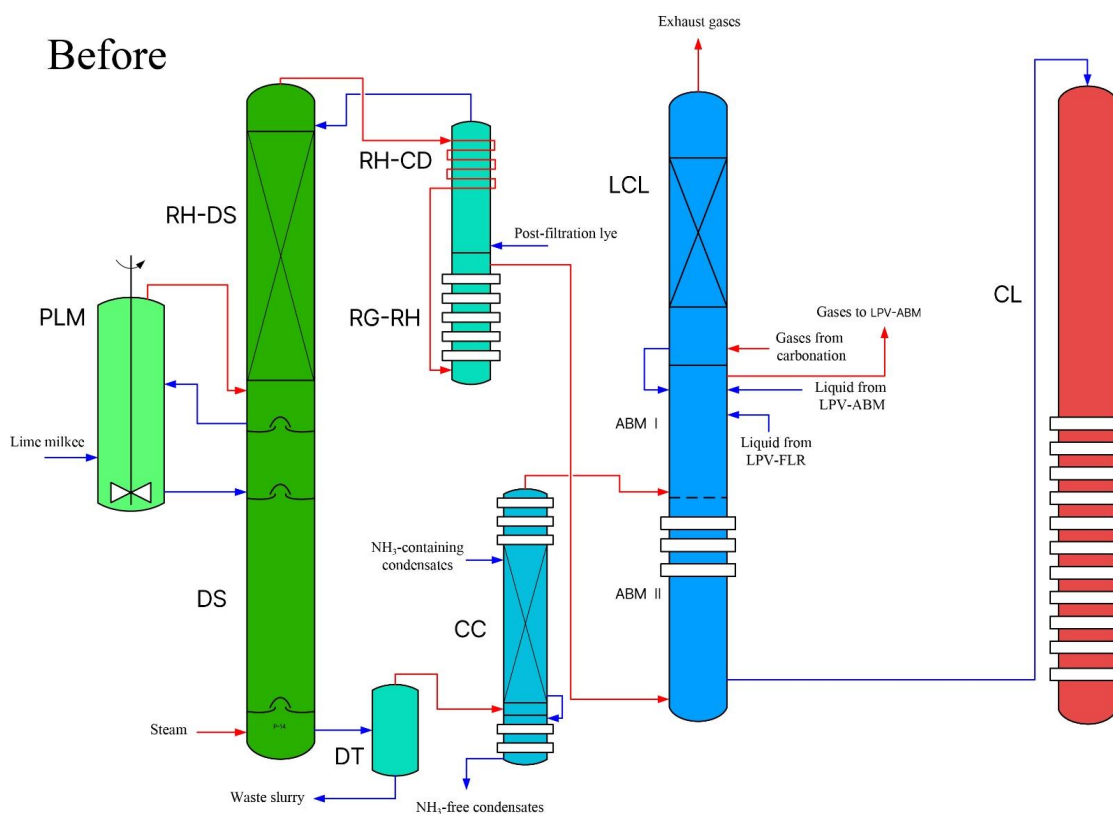


Figure 5. Traditional Solvay process absorption system implemented at CIECH Soda Polska S.A.'s Inowroclaw soda plants (based on [19]).

The process of making ammonia brine containing about $4.8 \text{ mol NH}_3 \cdot \text{dm}^{-3}$ in a saturating apparatus can be carried out with an ammonia concentration of up to $6.5 \text{ mol} \cdot \text{dm}^{-3}$. In view of the above, ammonia gases from the distillation process should be directed as a gas phase to a small countercurrent absorber with a cooler (SAB). Pre-carbonated ammonia brine is the absorbing liquid. The media are contacted in countercurrent. The cooled liquid after absorption is dispensed into the selected area of the carbonation column. A diagram of how the task is carried out is shown in Figure 6.

The choice of dosing sites for enriched ammonia brine to CL is a matter of research, which will be published in a subsequent paper. To properly characterize the procedure, the process of ammonia desorption from the system must also be analyzed. Ammonia desorption measurements were carried out to identify the ammonia loss in the sodium process for different ammonia concentrations in the starting solution, in an open system using our apparatus, shown in Figure 7.

Implemented

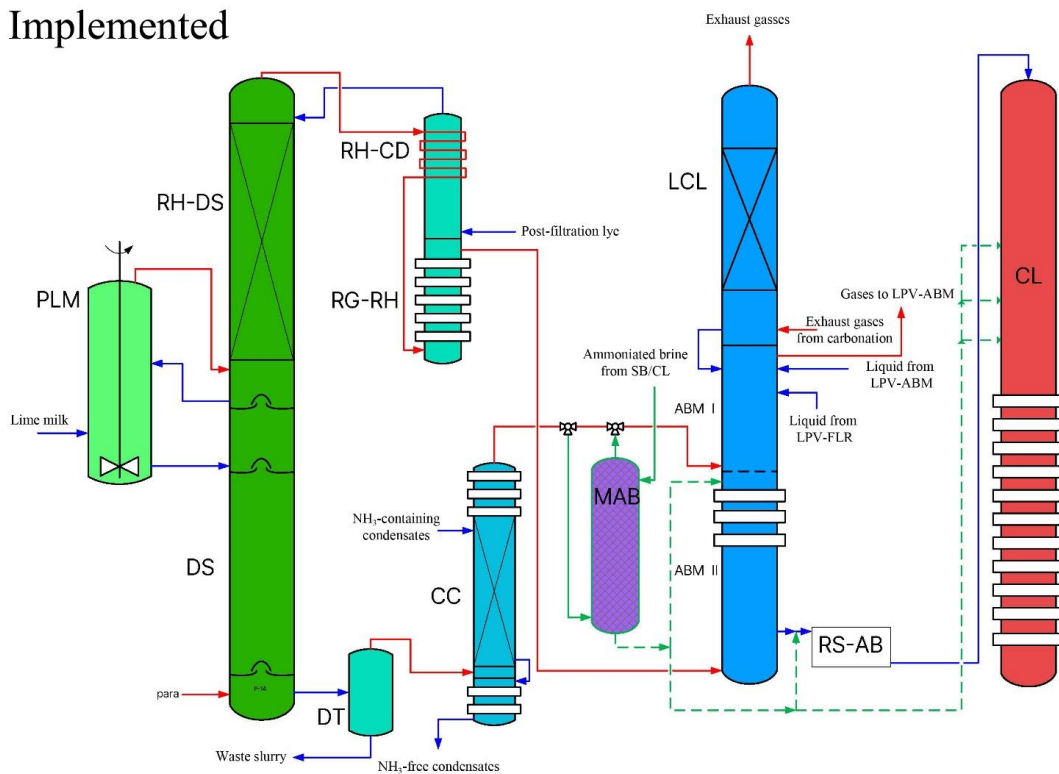


Figure 6. Modified Solvay process absorption system implemented at CIECH Soda Polska S.A.'s Inowrocław soda plants (based on [19]).

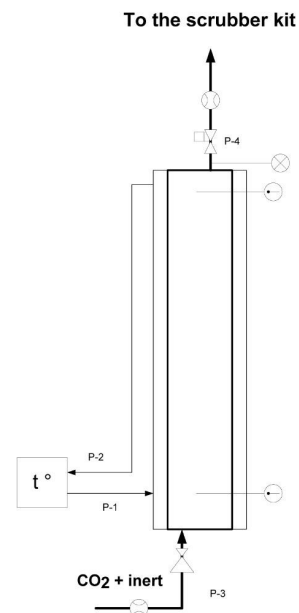


Figure 7. Ammonia desorption open system.

The apparatus made it possible to perform the tests at a strictly assumed volume rate of inert q_{in} , flowing from a buffer tank through a thermostated reactor containing a well-defined volume of ammonia brine of known chemical composition. The pressure and gas flow control block allowed full control of hydrodynamic parameters during the testing of the ammonia desorption process under intensive barbotage conditions in the reactor. The scrubber system, with a standard solution of sulfuric acid(VI) and sodium lye, provided measurements of the amount of ammonia and carbon dioxide in the effluent gas.

In order to determine the effect of the concentration of ammonia in the solution and the degree of carbonation on the intensity of the process under consideration, six solutions of ammonia brine with various chemical compositions were prepared: $C_{\text{NH}_3} = 4.404\text{--}6.258\text{mol}\cdot\text{dm}^{-3}$, $C_{\text{NaCl}} = 4.147\text{--}4.267\text{mol}\cdot\text{dm}^{-3}$, and $C_{\text{CO}_2} = 0.000\text{--}1.966\text{mol}\cdot\text{dm}^{-3}$.

An investigation of the ammonia desorption process at 303, 313, and 323 K was performed, analyzing the change in concentrations of ammonia, carbon dioxide, and sodium chloride in the liquid phase at specific time intervals.

Tables 2 and 3 list the measurement results of two series of tests of the kinetics of the ammonia desorption process with the extreme concentration of NH_3 in the brine.

Table 2. Effect of temperature, gas flow rate, and chemical composition of ammonia brine on ammonia desorption rate (experimental data).

Brine Chemical Composition of $c^{\circ}\text{NH}_3$ $c^{\circ}\text{NaCl}$ $c^{\circ}\text{CO}_2$ ($\text{mol}\cdot\text{dm}^{-3}$)/($\text{mval}/20\text{ cm}^3$)	Ammonia Concentration in $c^{\text{I}}\text{NH}_3$ Solution	Temperature T (K)					
		303		313		323	
		Gas flow Rate ($q_{\text{in}}\text{ dm}^3\text{ h}^{-1}$)					
		8.0	12.0	8.0	12.0	8.0	12.0
		Desorption Time					
		t (s)					
1	2	3	4	5	6	7	8
4.404/88.08	4.404/88.08	0	0	0	0	0	0
4.267/85.34	4.286/85.72	665	370	380	190	175	100
0.000/0.00	4.167/83.34	1210	740	765	385	350	200
	4.048/80.96	1765	1090	1095	605	515	305
	3.930/78.60	2320	1490	1460	800	685	415
4.394/87.88	4.394/87.88	0	0	0	0	0	0
4.247/84.94	4.276/85.52	1100	680	610	525	425	200
0.953/38.12	4.157/83.14	2190	1330	1165	1025	920	385
	4.038/80.76	3355	2035	1740	1640	1330	560
	3.920/78.40	4565	2705	2355	2215	1775	772
4.384/87.68	4.384/87.68	0	0	0	0	0	0
4.217/84.34	4.266/85.32	1270	890	940	570	502	360
1.375/55.00	4.147/82.94	2470	1770	1870	1125	989	658
	4.028/80.56	3640	2650	2790	1715	1559	1163
	3.910/78.20	4880	3675	3800	2270	2101	1541

Table 3. Effect of temperature, gas flow rate, and chemical composition of additionally ammoniated brine on ammonia desorption rate (experimental data).

Brine Chemical Composition of $c^{\circ}\text{NH}_3$ $c^{\circ}\text{NaCl}$ $c^{\circ}\text{CO}_2$ ($\text{mol}\cdot\text{dm}^{-3}$)/($\text{mval}/20\text{ cm}^3$)	Ammonia Concentration in $c^{\text{I}}\text{NH}_3$ Solution	Temperature T (K)					
		303		313		323	
		Gas Flow Rate ($q_{\text{in}}\text{ dm}^3\text{ h}^{-1}$)					
		8.0	12.0	8.0	12.0	8.0	12.0
		Desorption Time					
		t (s)					
1	2	3	4	5	6	7	8
6.258/125.2	6.258/125.2	0	0	0	0	0	0
4.148/82.96	6.140/122.8	460	275	222	140	120	85
0.000/0.00	6.021/120.4	980	550	455	275	250	170
	5.902/118.0	1350	780	690	415	370	250
	5.784/115.7	1720	1080	910	550	500	340
6.175/123.5	6.175/123.5	0	0	0	0	0	0
4.147/82.94	6.057/121.1	520	345	370	245	205	145
1.265/50.6	5.938/118.8	1030	685	715	495	420	295
	5.819/116.4	1565	1030	1090	730	615	440
	5.701/114.0	2095	1385	1460	980	815	590
6.141/122.8	6.141/122.8	0	0	0	0	0	0
4.209/84.18	6.041/120.8	665	475	500	370	330	240
1.966/78.64	5.903/118.1	1335	940	990	755	670	490
	5.785/115.7	1990	1340	1485	1105	995	725
	5.666/113.3	2665	1795	1995	1470	1315	965

In the following, we summarize the chemical composition of the ammonia brine entering the reactor, the change in concentration of total ammonia in solution, the temperature of the process, the value of the volumetric flow rate of the inert gas, and the time of ammonia desorption.

The effect of individual process parameters on the studied ammonia desorption was evaluated by function analysis:

$$K_{\text{NH}_3}^{\text{des}} = f(T, R, c_{\text{NH}_3\text{c}}^{\text{O}}, q_{\text{in}}) \quad (16)$$

Within the studied range of temperature changes, ammonia brine chemistry, and inert volume flow rate, the desorption intensity of NH_3 was approximated by the equation:

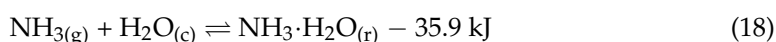
$$N_{\text{NH}_3}^{\text{des}} = K_{\text{NH}_3}^{\text{des}} \cdot c_{\text{NH}_3\text{c}} \quad (17)$$

The experimental data of the desorption process confirm the assumptions of the kinetics of this process. The higher the temperature, the greater the desorption. Because the stream of desorbed ammonia is not linear, experimental studies of the desorption rate were conducted. The desorption tests confirmed that in order for additional ammonia to be bound, it must be dosed to the zone of the carbonation column, where the total CO_2 concentration is as high as possible. As a result, the desorption time will be the longest and the concentration of carbamate ions the highest. Research on this process was carried out at the Faculty of Chemistry of the Nicolaus Copernicus University in Toruń.

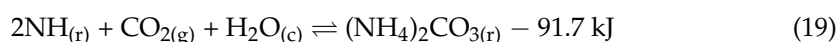
4. Solution Implementation and Energy Changes

In order to implement the ammonization process of ammonia brine and pre-carbonated ammonia brine using the SAB plant, a number of technical, technological, and analytical experiments were carried out. In the course of the work, a well-defined flux of ammoniated brine was obtained with direct alkalinity of $130\text{--}140 \text{ mmol} \cdot 20 \text{ cm}^{-3}$ (i.e., $6.50\text{--}7.00 \text{ mol} \cdot \text{dm}^{-3}$).

In the course of the work, favorable conditions were created to carry out the research on a higher concentration of ammonia in the brine, and thus a higher concentration of CO_2 and the co-crystallization of NH_4HCO_3 or NaCl . The absorption of ammonia in aqueous solution can be represented by the following equation:



The absorption of carbon dioxide in an aqueous ammonia solution can be presented as follows:



Ammonia is a gas that is easily soluble in water. In this case, the absorption of the gas in water is affected only by the resistance of the gas boundary layer. The rate of this process can be expressed by the formula:

$$N = K_g S (P_g - P_r) \text{ (kmol} \cdot \text{h}^{-1} \cdot \text{m}^{-2}\text{)} \quad (20)$$

The expression $(P_g - P_r)$ is referred to as the driving force of the absorption process, or absorption potential. This potential depends on the partial pressure difference of the absorbate (P_g) in the feed gas and its equilibrium pressure over the liquid (P_r). These values are expressed in mm Hg. In the above equation, K_g expresses the absorption constant in the gaseous boundary layer, the unit of which is $\text{kmol} \cdot \text{m}^{-2} \cdot \text{h}^{-1} \cdot \text{mmHg}^{-1}$. For the product of $K_g S$, an approximation is assumed, which leads to a constant value during the absorption process at each stage under certain conditions. Given this assumption, it can be concluded that the rate of absorption is affected only by the value of the potential. The matter gets a bit more complicated if we also take into account the influence of CO_2 . As can be seen from the above reaction equations, the absorption of both components into the liquid causes an exoenergetic reaction, which results in the release of heat and ultimately

an increase in the temperature of the solution. This adversely affects the equilibrium pressure of carbon dioxide, by which its absorption efficiency decreases. An increase in temperature significantly accelerates the rate of reaction and reduces the viscosity of the solution, causing favorable conditions for ammonia diffusion, thereby facilitating the absorption of CO₂ according to the chemical reaction. To avoid this, it was assumed that the absorption process would take place at an elevated temperature not exceeding 343 K.

The basic factors that guided the design, construction, and operation of the SAB absorber were as follows:

- Method of conducting the process, continuous or semi-continuous;
- Mass exchange area;
- Liquid retention time;
- Determination of the phase that controls the speed of the process;
- Exoenergetic process: heat removal, use of cooling;
- Probability of corrosion of apparatus; and
- Rate of gas and liquid flow entering the apparatus.

The implementation of the task was carried out according to the layout shown in Figures 6 and 8.

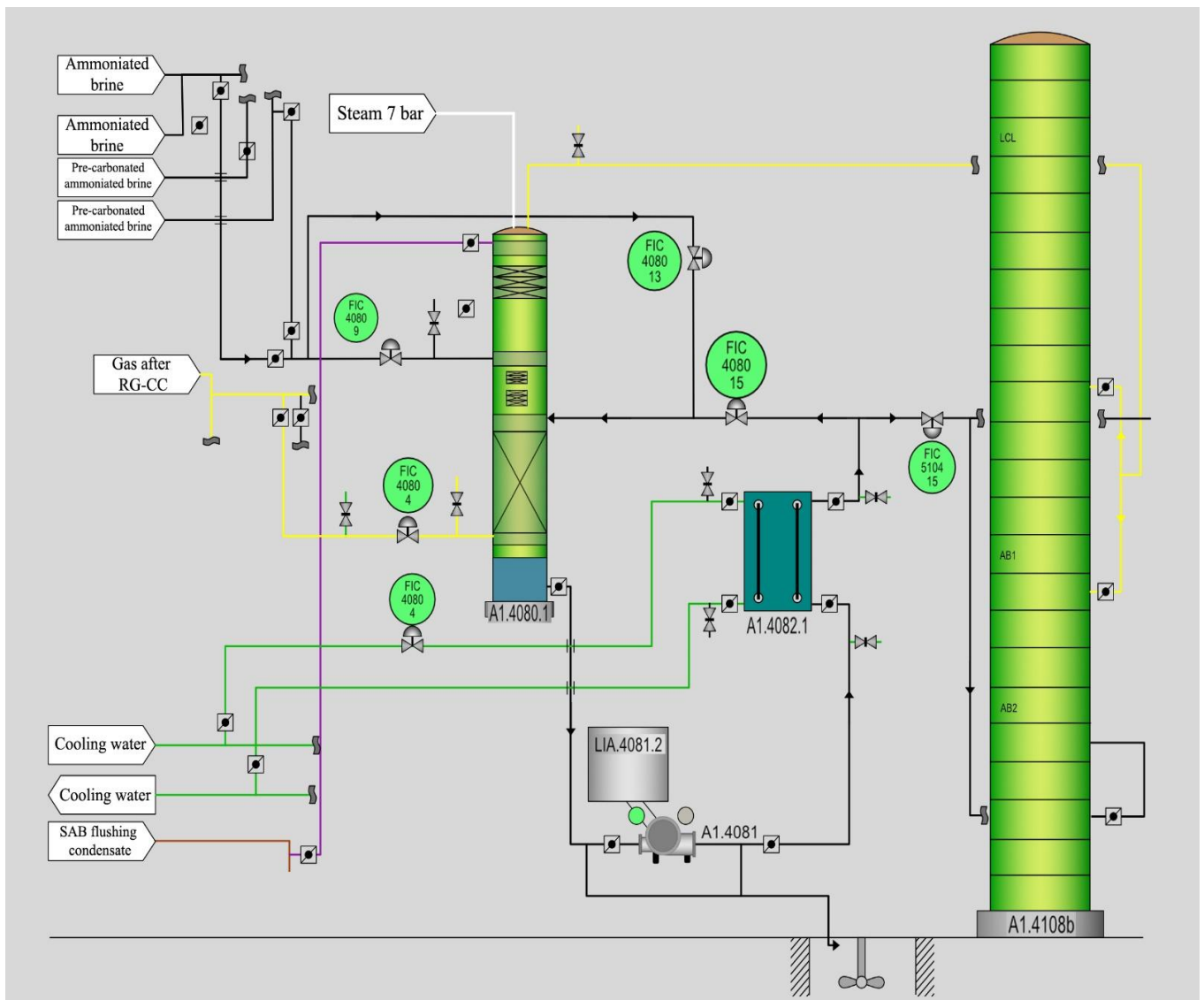


Figure 8. Coupled system to conduct the amonization process (SAB).

The basic scheme of the apparatus was rearranged in the following manner. Gas after RG-CC (FIC 4080.4) was introduced into the countercurrent SAB absorber, with Pall fill and cellular fill at the top of the apparatus, in countercurrent to the brine solution introduced through two stubs: onto the cellular fill (FIC 4080.9) and onto the Pall fill (FIC 4080.13), with the flux directed onto the Pall fill connected to the return flux (FIC 4080.15). The waste gas was directed to the corresponding absorber.

The ammoniated brine was directed to the cooler (A1.4082.1), from which the stream was divided into two parts: the turnback (FIC 4080.15), which is part of the flux directed to the Pall fill, and the flux of ammoniated brine (FIC 5104.15), which is directed in the start-up and test stage to the absorber tank, and in the carbonation stage to the corresponding CL location. The parameters of the SAB were as follows: The column was installed at +9900, designed as an apparatus consisting of three segments and a gas discharge head. The diameter and height of the apparatus were $D = 1000$ mm and $H = 8000$ mm. In the lower segment, there was a brine tank with a volume of $V = 0.78$ m³, above which is a pre-absorption zone on a bed of Pall rings with a contact area of 240 m². The filling in the lower segment had the following characteristics: Pall rings, $50 \times 50 \times 2$, 316 L, $V = 1.80$ m³. In the middle segment, flow was designed through two layers of cellular fill. Absorption of about 65% of the ammonia contained in the gas after passing through the Pall rings was assumed on the cellular fill. The characteristics of the fill in the middle segment were as follows: process cell fill of 2×3 layers, 316 L, ϕ 600. The apparatus was designed so that it would also be possible to remove the cell fill and replace it with another bed of Pall rings.

In the upper segment of the column was a designed demister, comprising a separation cell fill of three layers, 316 L, ϕ 600. A tray was placed under the column, from which all possible leaks from the stubs of the column could be drained by gravity.

The implementation of the SAB operation was carried out in such a way that the gas was started first and the brine flow was second. Once the flows were established, the appropriate amount of cooled brine per turn was determined and the process parameters were observed.

The research objective of the absorption process was to determine the motion parameters of the SAB absorber, in particular the relationship of total alkalinity = $f(V$ brine V1, V brine V2) (Figures 9 and 10), and the parameters under production conditions.

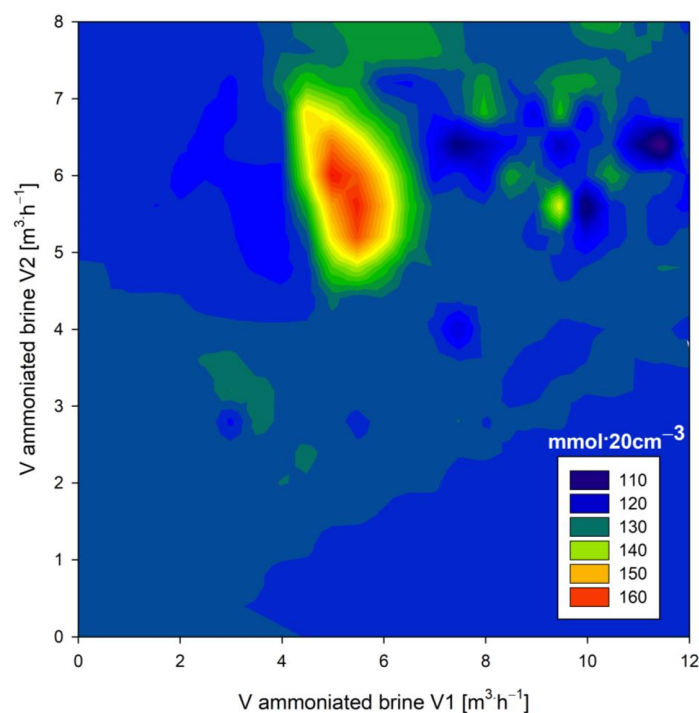


Figure 9. Total alkalinity dependent on V1 and V2 streams.

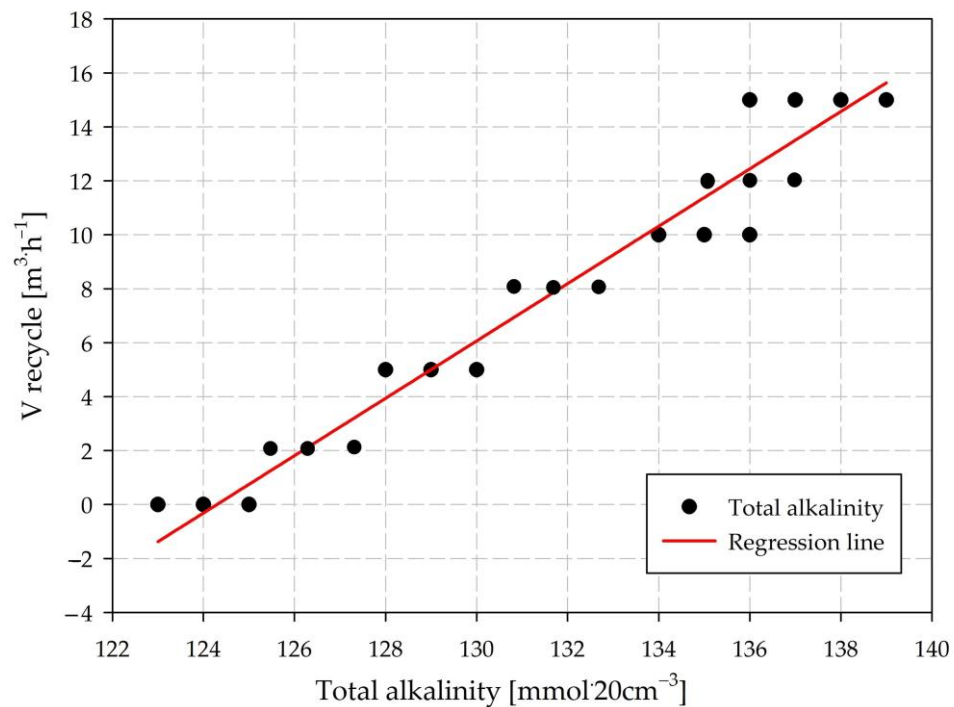


Figure 10. Total alkalinity dependent on V_{recycle} stream.

The analysis of the data, presented in Figure 9, allowed us to determine the optimal volume ratio for SAB liquids in order to obtain the highest possible alkalinity. The green-red area is optimal. For the selected area in Figure 9, the volume of the recycle stream was determined. From Figure 10, it can be concluded that in the range of 124–135 $\text{mmol} \cdot 20 \text{ cm}^{-3}$, it increased linearly. The volume of the recycle stream (except from the recycle stream temperature) may be a parameter for controlling the direct alkalinity of the additional ammoniated brine.

The carbamate ion concentration is responsible for the increase in efficiency of the carbonation process. As seen in the results of the data presented in Table 4, the concentration of carbamate ions increased significantly during the addition of ammonification, while the parameters of the brine were maintained. The higher alkalinity due to the higher concentration of ammonia caused a greater fixation of the CO_2 contained in the reaction solution. Increasing the concentration of NH_2COO^- ions caused an increase in supersaturation in the crystallization area of NaHCO_3 . This effect is very favorable for the efficiency of the soda process.

Table 4. Results of analysis of and calculations for ammoniated brine.

Analyte ($\text{mval} \cdot 20 \text{ cm}^{-3}$)	Brine after SAB					Brine before SAB
	1	2	3	4	5	
$a \equiv [\text{NH}_3]$	130.6	132.8	135.0	129.1	126.6	98.9
$c \equiv [\text{Cl}^-]$	83.1	81.1	80.9	81.2	80.8	87.6
$q \equiv [\text{Na}^+]$	83.1	81.1	80.9	81.2	80.8	87.6
$m \equiv [\text{NH}_3(\text{r})]$	54.4	55.3	81.9	103.4	76.9	79.7
$n \equiv [\text{alkalinity}]$	130.6	132.8	135.0	129.1	126.6	98.9
$o \equiv [\text{NH}_4^+]$	49.5	50.3	36.1	19.3	34.3	12.9
pH	9.61	9.62	9.93	10.30	9.92	9.40
$d \equiv [\text{CO}_2]$	78.3	79.7	54.0	25.8	50.6	19.8
$w \equiv [\text{CO}_3^{2-}] + [\text{HCO}_3^-] + [\text{CO}_2(\text{r})]$	25.1	25.2	20.1	13.4	19.7	7.3
$e \equiv [\text{NH}_2\text{COO}^-]$	53.2	54.5	33.9	12.4	30.9	12.5
$f \equiv [\text{CO}_3^{2-}]$	20.7	20.8	18.3	12.9	17.9	6.0
$g \equiv [\text{HCO}_3^-]$	4.4	4.4	1.9	0.56	1.9	1.3
$k \equiv [\text{acidity}]$	78.33	79.7	54.0	25.8	50.6	19.8
l (ionic force)	197.2	198.4	168.9	129.5	165.9	95.8

Process energy changes are best presented in the form of a Sankey diagram [20,21]. The energy effect of the carbonation process is presented in Figure 11.

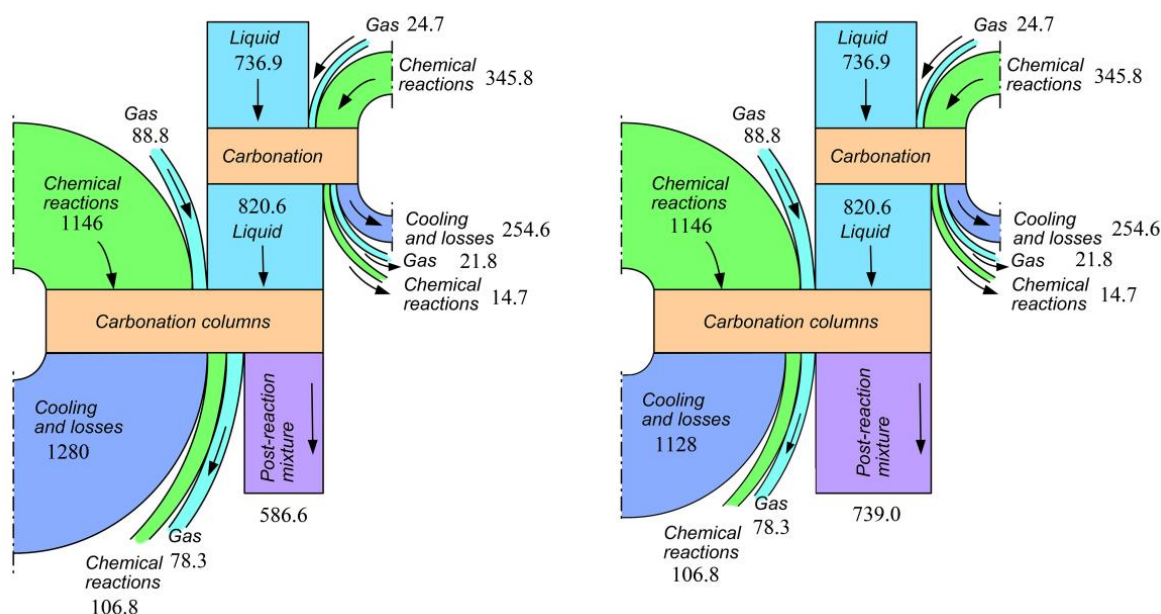


Figure 11. Energetic effects of soda in carbonation process, in MJ·Mg⁻¹.

In the experiment, after increasing the concentration of ammonia in the carbonation process, there was an increase in temperature at the exit from the column. The efficiency of the soda process increased slightly, due to the suction effect on NaHCO₃. This also has a beneficial effect on the process in summer conditions, when it is difficult to cool the carbonation column.

From the data presented in Table 4, it can be seen that the composition of the ammoniated brine strictly depends on the composition of the absorbed gas, and in particular on the amount of NH₃ and CO₂ in the gas fed into the SAB. The fact that the amount of CO₂ in the gas after RG-CC translates directly into the amount of carbamate ions in the solution after SAB should receive special attention.

For the carbonation process, ammoniated brine solutions containing the highest possible concentration of NH₂COO⁻ ions are preferred, which will cause a direct increase in supersaturation in CL.

5. Environmental Aspects

Minimized cooling water consumption resulting from the reduced cooling by 152.4 MJ·Mg⁻¹ was the main effect of the change in process regime. An additional ecological effect is presented in Figure 12. The concentrations of CO₂ and NH₃ in the exhaust gas were measured by infrared absorption using an LDS-6 laser process gas analyzer (Siemens, Germany). The diagram shows that during dosing of additional ammoniated brine, the CO₂ and NH₃ concentrations in the exhaust gases decreased. Additional ammoniated brine dosing was alternated with periods of no dosing. The CO₂ concentration exceeded 25% v/v without additional ammoniated brine and was on average 3.85% lower with ammoniated brine. Likewise, the concentration of NH₃ was 0.63% lower on average. Lowering the concentration of CO₂ and NH₃ in the waste gas has a very large ecological benefit in terms of total NaHCO₃ production.

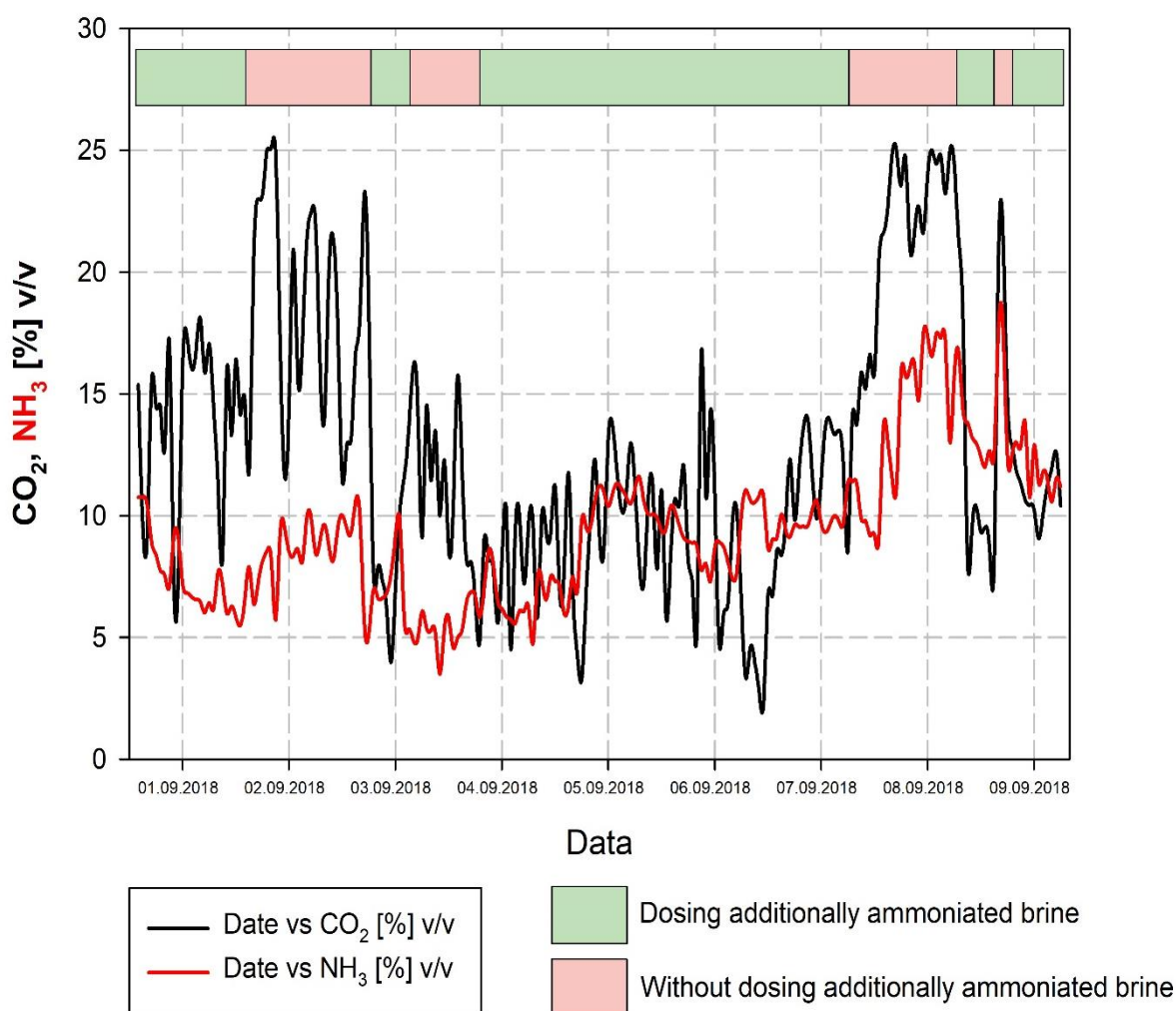


Figure 12. Concentrations of CO₂ and NH₃ in carbonation column exhaust gases.

As a result of extensive analytical and industrial research at CIECH Soda Polska S.A.'s Inowrocław soda plants using ammoniated brine, the soda yield of the process was increased using the developed SAB device. Acknowledging that the soda industry is troublesome in terms of waste [1,16,18], this reduction in the amount of substrate at higher yields also minimizes the amount of process by-product. An additional environmental aspect, due to the thermodynamics of the process, is the increase in temperature at the outlet of the carbonation column, with unchanged crystal quality. This results in minimized cooling water consumption, which minimizes the cost of producing NaHCO₃.

6. Conclusions

The study shows that the rate of ammonia desorption increases exponentially with increasing temperature and inert volumetric flow rate, while it decreases with increasing carbonation of the system. The value of the kinetic constant of the ammonia desorption process at an inert volume flow rate of 8.0 dm³·h⁻¹ varied in the range 2–24 × 10³ mmol·dm⁻³·s⁻¹, while at a volumetric flow rate of 12.0 dm³·h⁻¹ the range was 4–27 × 10³ mmol·dm⁻³·s⁻¹. The above relationships provide the basis for determining the optimal range of process parameters for the initial carbonation of ammonia brine using Solvay technology. Considering the hydrodynamic data of the SAB absorber, after conducting a series of experiments, the results of which are presented above, it can be assumed that the model parameters of the system are as follows: Average flux of pre-carbonated brine directed to the Pall fill (V2) is about 8 m³·h⁻¹; average flux of pre-carbonated brine directed to the cell fill (V1) is about 12 m³·h⁻¹; average turning flux is about 10 m³·h⁻¹; and increase in total

alkalinity is about $36 \text{ mmol} \cdot 20 \text{ cm}^{-3}$. The increase in overall CO_2 in ammoniated brine can be described by the relation: $y = 0.86x - 29.2$ where y is overall CO_2 and x is general alkalinity; the average gas flow for the above streams is about $2800 \text{ Nm}^3 \cdot \text{h}^{-1}$. The MAB operating temperature is 334–340 K, and the mass exchange flux of ammonia between gas phase and liquid is $61.2 \text{ kg NH}_3 \cdot \text{h}^{-1} \cdot \text{m}^{-3}$; thus, this is the value of the transfer coefficient of ammonia under fixed hydrodynamic conditions. The temperature of the bottom of the carbonation column may be 307 K without additional cooling. This saves energy due to the need for less cooling water.

Author Contributions: Conceptualization, M.C. and L.K.; methodology, M.C. and B.K.; software, L.K. and S.L.; validation, B.K., D.Ž. and M.S.; formal analysis, M.C. and B.K.; data curation, K.S.; writing—original draft preparation, M.C.; writing—review and editing, U.K.; visualization, S.L.; supervision, U.K.; project administration, M.S. All authors have read and agreed to the published version of the manuscript.

Funding: This work was carried out within a development project by CIECH R&D in cooperation with Nicolaus Copernicus University in Toruń (subcontractor) on a world innovative technology for the carbonation of ammonia brine enabling an increase in the soda yield of the soda ash production process (POIR.01.02.00-0031/2016) co-financed within Operational Programme Smart Growth 2014–2020, Measure 1.2. Sectoral R&D programs. Special thanks go to the Bialystok University of Technology Faculty of Construction and Environmental Sciences for facilitating the calculations.

Data Availability Statement: Data sharing is not applicable to this article.

Acknowledgments: Special thanks go to the Bialystok University of Technology Faculty of Construction and Environmental Sciences for facilitating the calculations.

Conflicts of Interest: The authors declare no conflict of interest.

Abbreviations

PLM	lime mixer (pre-limer)
RH-DS	distiller heater
DS	distiller
RH-CD	diaphragm filter liquor heater
RG-RH	ammonia regeneration node gas cooler
DT	distiller liquid expander (detander)
CC	ammonia distillation column from condensates
MAB	small absorber (enrichment of ammonia brine into ammonia)
LCL	carbonation gas scrubber
ABM I	absorber upper part
ABM II	absorber lower part
SA	ammonia brine
SB–CL (SB/CL)	scrubber of column gases
LPV–FLR	filter gas scrubber to vacuum pump
LPV–ABM	absorber gas scrubber to vacuum pump
RS–AB	brine tank after ammonia absorption
CL	settling (production) carbonation column
SAB	small absorber (solution being implemented)
V	flow rate of the gaseous phase
K	overall mass exchange coefficient
$K_v = K \cdot \Delta$	Δ is the size of phase separation area per unit volume
F_0	cross-sectional area of column
X_{up}, X_{down}	ammonia content of input and output liquid from SAB
Y_{up}, Y_{down}	ammonia content of input and output gas from SAB
L_{up}, L_{down}	volume of liquid flow per unit time, input and output from SAB
G_{up}, G_{down}	volume of gas flow per unit time, input and output from SAB

G	amount of substance passing from one phase to another
F	size of phase separation area
Δy	driving force of mass exchange process, i.e., difference between actual concentration of a substance in a given phase and its achievable concentration at equilibrium
y	actual concentration of substance in a specific phase
y^*	concentration of substance in same phase at equilibrium
y_1	absorbate concentration in gas phase before absorption
y_2	absorbate concentration in gas phase after absorption
Δy_{sr}	mean driving force
H_w	column fill height
L	liquid flow rate ($\text{kg}\cdot\text{s}^{-1}$)
k_x	mass penetration coefficient for liquid film ($\text{kg}\cdot\text{m}^{-2}\cdot\text{s}^{-1}$)
a	area of filling unit ($\text{m}^2\cdot\text{m}^{-3}$)
S	cross-sectional area of column (m^2)
q_{in}	specific flow of inertia
$K_{\text{NH}_3}^{des}$	ammonia desorption rate constant ($\text{mmol}\cdot\text{dm}^{-3}\cdot\text{s}^{-1}$)
R	degree of carbonation of solution
$C_{\text{NH}_3c}^0$	initial concentration of ammonia in working liquid
$c^t\text{NH}_3$	concentration of ammonia in liquid after time t
P_g	partial pressure of absorbate
P_r	equilibrium pressure of adsorbate over liquid
K_g	absorption constant in gaseous boundary layer ($\text{kmol}\cdot\text{m}^{-2}\cdot\text{h}^{-1}\cdot\text{mmHg}^{-1}$)
V_{max}	maximum flow per unit time
C_{NaCl}	sodium chloride concentration
T	temperature
t	time
a	$[\text{NH}_3]$ total ammonia concentration, compliant with ISO 21877
c	$[\text{Cl}^-]$ chloride concentration, compliant with ISO 5314:1981
q	$[\text{Na}^+]$ sodium concentration, compliant with BN-90 9567-29
m	$[\text{NH}_{3(\text{aq})}]$ free ammonia concentration physically dissolved in solution
n	[alkalinity] total concentration of alkaline compounds, compliant with ISO 9963-1
o	$[\text{NH}_4^+]$ modification of ISO 5314:1981
d	$[\text{CO}_2]$ total concentration of carbon dioxide in solution, compliant with Standard Method 4500-CO ₂ Carbon Dioxide (2017)
w	$[\text{CO}_3^{2-}] + [\text{HCO}_3^-] + [\text{CO}_2(\text{r})]$ total concentration of carbonates and free carbon dioxide
e	$[\text{NH}_2\text{COO}^-]$ carbamate ion concentration, NMR and precipitation methods
f	$[\text{CO}_3^{2-}]$ carbonate ion concentration, compliant with EN ISO 10693:2014
g	$[\text{HCO}_3^-]$ hydrocarbonate concentration, compliant with EN ISO 10693:2014
I	ionic force
W_{Na}	sodium yield of process

References

1. Cichosz, M.; Igliński, B.; Buczkowski, R.; Rzymyszkiewicz, P. Rozwój i stan przemysłu sodowego na świecie. *Przemysł Chem.* **2018**, *3*, 319–325. [\[CrossRef\]](#)
2. Kang, Z.; Jia, X.; Zhang, Y.; Kang, X.; Ge, M.; Liu, D.; Wang, C.; He, Z. A Review on Application of Biochar in the Removal of Pharmaceutical Pollutants through Adsorption and Persulfate-Based AOPs. *Sustainability* **2022**, *14*, 10128. [\[CrossRef\]](#)
3. Zahmatkesh, S.; Amesho, K.T.T.; Sillanpaa, M.; Wang, C. Integration of renewable energy in wastewater treatment during COVID-19 pandemic: Challenges, opportunities, and progressive research trends. *Clean. Chem. Eng.* **2022**, *3*, 100036. [\[CrossRef\]](#)
4. Liu, Z. National carbon emissions from the industry process: Production of glass, soda ash, ammonia, calcium carbide and alumina. *Appl. Energy* **2016**, *166*, 239–244. [\[CrossRef\]](#)
5. Li, C.; Liang, Y.; Jiang, L.; Zhang, C.; Wang, Q. Characteristics of ammonia-soda residue and its reuse in magnesium oxychloride cement pastes. *Constr. Build. Mater.* **2021**, *300*, 123981. [\[CrossRef\]](#)
6. Wang, X.-b.; Yan, X.; Li, X.-y. Environmental risk for application of ammonia-soda white mud in soils in China. *J. Integr. Agric.* **2020**, *19*, 601–611. [\[CrossRef\]](#)

7. Cormos, A.-M.; Cormos, C.-C.; Agachi, P.Ş. Making soda ash manufacture more sustainable. A modeling study using ASPEN Plus. In *Computer Aided Chemical Engineering*; Pleşu, V., Agachi, P.Ş., Eds.; Elsevier: Amsterdam, The Netherlands, 2007; Volume 24, pp. 551–556.
8. Zahmatkesh, S.; Klemeš, J.J.; Bokhari, A.; Rezakhani, Y.; Wang, C.; Sillanpaa, M.; Amesho, K.T.T.; Ahmed, W.S. Reducing chemical oxygen demand from low strength wastewater: A novel application of fuzzy logic based simulation in MATLAB. *Comput. Chem. Eng.* **2022**, *166*, 107944. [[CrossRef](#)]
9. Hou, T.-P. *Manufacture of Soda*; Reinhold Publishing Corporation: New York, NY, USA, 1942.
10. Zarzycki, R.C.A.; Coulson, J.M. *Absorption Fundamentals and Applications*; Pergamon Press: Oxford, UK; New York, NY, USA; Seoul, Korea; Tokyo, Japan, 1993; p. 647.
11. Chu, F.; Yang, L.; Du, X.; Yang, Y. Mass transfer and energy consumption for CO₂ absorption by ammonia solution in bubble column. *Appl. Energy* **2017**, *190*, 1068–1080. [[CrossRef](#)]
12. Brian, P.L.T.; Hurley, J.F.; Hasseltine, E.H. Penetration theory for gas absorption accompanied by a second order chemical reaction. *AIChE J.* **1961**, *7*, 226–231. [[CrossRef](#)]
13. Fedotieff, P.P. Der Ammoniak sodaprozess vom Standpunkte der Phasenlehre. *Z. Phys. Chem.* **1904**, *49U*, 162–188. [[CrossRef](#)]
14. Qin, F.; Wang, S.; Hartono, A.; Svendsen, H.F.; Chen, C. Kinetics of CO₂ absorption in aqueous ammonia solution. *International J. Greenh. Gas Control* **2010**, *4*, 729–738. [[CrossRef](#)]
15. Mann, R.; Moyes, H. Exothermic gas absorption with chemical reaction. *AIChE J.* **1977**, *23*, 17–23. [[CrossRef](#)]
16. Fortescue, G.E.; Pearson, J.R.A. On gas absorption into a turbulent liquid. *Chem. Eng. Sci.* **1967**, *22*, 1163–1176. [[CrossRef](#)]
17. Cichosz, M.; Kielkowska, U.; Skowron, K.; Kiedzik, L.; Łazarski, S.; Szkudlarek, M.; Kowalska, B.; Żurawski, D. Changes in Synthetic Soda Ash Production and Its Consequences for the Environment. *Materials* **2022**, *15*, 4828. [[CrossRef](#)] [[PubMed](#)]
18. Onda, K.; Sada, E.; Kobayashi, T.; Fujine, M. Gas absorption accompanied by complex chemical reactions—III Parallel chemical reactions. *Chem. Eng. Sci.* **1970**, *25*, 1023–1031. [[CrossRef](#)]
19. Skowron, K.; Sobczak, W.; Kiedzik, L.; Zelazny, R.; Buczkowski, R.; Wachowiak, M.; Cichosz, M. Method for Brine Carbonization with Additional Amount of Ammonia in a Process of Soda Production and System of Devices for Carrying Out This Method. European Patent EP3312143A1, 19 October 2017.
20. de-Córdoba, G.F.; Molinari, B. Sankey diagrams for macroeconomics: A teaching complement bridging undergraduate and graduate Macro. *Heliyon* **2022**, *8*, e10717. [[CrossRef](#)] [[PubMed](#)]
21. Glover, R.E.; Al-Haboubi, M.; Petticrew, M.P.; Eastmure, E.; Peacock, S.J.; Mays, N. Sankey diagrams can clarify ‘evidence attrition’: A systematic review and meta-analysis of the effectiveness of rapid diagnostic tests for antimicrobial resistance. *J. Clin. Epidemiol.* **2022**, *144*, 173–184. [[CrossRef](#)]